




Choline-based ionic liquids enhance the dermal delivery of cyclosporine a for potential treatment of psoriasis

Yang Li¹ · Qin Yu^{1,2} · Yi Lu^{1,2,4} · Yanyun Ma⁴ · Jianping Qi^{1,2} · Zhongjian Chen² · Quangang Zhu² · Wei Wu^{1,2,3,4} 

Accepted: 26 August 2024
© Controlled Release Society 2024

Abstract

Psoriasis is a prevalent chronic disease affecting 2–3% of the global population. Cyclosporine A (CyA) has been widely used with great promise in the treatment of moderate to severe psoriasis despite various side effects associated with its systemic administration. Topical administration of CyA circumvents systemic side effects; however, the poor water solubility and large molecular weight of CyA pose challenges for dermal delivery. In this study, choline-based ionic liquids (ILs) were used to enhance the dermal delivery of CyA for the potential treatment of psoriasis. All four ILs tested significantly improved the solubility of CyA, which was greater than that of the control group with dimethyl sulfoxide (DMSO) as a solubilizer (20%, w/w). The saturated solubility of CyA in two of the ILs, choline geranate ([Ch][Ge]) and choline ricinoleate ([Ch][Ra]), reached more than 90 mg/mL, and the solubilization capability of the ILs except [Ch][Ci] was resistant to water dilution. The negligible change in CyA content determined by high-performance liquid chromatography and the secondary structure detected by circular dichroism spectroscopy confirmed the stability of CyA in the ILs. At 4 h in the *in vitro* penetration test, the amount of CyA retained in the skin in the IL groups was slightly greater than that in the control group (20% DMSO). The water content of the ILs significantly affected their penetration ability. When the water content increased from 10 to 70%, the dermal delivery of CyA first increased, peaked at a water content of 30%, and then decreased. The dermal delivery ability of [Ch][Ge] and [Ch][Ra] with a water content of 70% was still comparable to that of 20% DMSO. Moreover, CyA-loaded ILs (0.5%, w/w) significantly relieved the symptoms of psoriasis in an imiquimod (IMQ)-induced mouse model, and the levels of inflammatory factors, including tumor necrosis factor α , interleukin 22 and interleukin 17, in the affected area were reduced by 71.7%, 75.6%, and 89.3%, respectively. The IL tested, choline sorbate ([Ch][So]), showed low cytotoxicity to human immortalized epidermal cells (HaCaT). After 7 days of consecutive application, [Ch][So] did not cause significant irritation. In conclusion, ILs demonstrate promising potential for the dermal delivery of CyA for the treatment of psoriasis.

Keywords Ionic liquids · Choline · Cyclosporine A · Psoriasis · Drug delivery · Dermal delivery

Yang Li and Qin Yu contributed equally to this work.

✉ Quangang Zhu
qgzhu@126.com

✉ Wei Wu
wuwei@shmu.edu.cn

¹ School of Pharmacy, Key Laboratory of Smart Drug Delivery, Fudan University, Ministry of Education, Shanghai 201203, China

² Shanghai Skin Disease Hospital, Tongji University School of Medicine, Shanghai 200443, China

³ Center for Medical Research and Innovation, Shanghai Pudong Hospital, Fudan University Pudong Medical Centre, Shanghai 201399, China

⁴ Fudan Zhangjiang Institute, Shanghai 201203, China

Introduction

Psoriasis is a common, long-term skin disorder that affects approximately 2–3% of the global population [1]. Although the exact cause of psoriasis remains unclear, it is widely believed that T cells are likely involved in the development of psoriasis [2]. Psoriasis patients suffer from scaly skin due to inflammatory infiltration and keratinocyte hyperproliferation. Immunosuppressive agents are currently the remedies of choice for psoriasis treatment [3]. Cyclosporine A (CyA), a calcineurin inhibitor, was chosen as a safe and effective medication for this purpose at the 2008 National Psoriasis Foundation Consensus Conference [4]. To date, only oral formulations of CyA, such as Neoral[®], Neocypsin[®], and

Sandimmune[®], are clinically available for the treatment of psoriasis [5, 6]. However, the oral administration of CyA is associated with many side effects, including systemic nephrotoxicity and arthritis, and this treatment is prescribed only for severe conditions involving large areas of psoriasis [4, 7]. Topical administration applies CyA directly to the affected skin surfaces, thus reducing side effects associated with systemic administration [8–10]. However, owing to its low solubility and large molecular weight (1202.6 g/mol), CyA encounters difficulties in permeating stratum corneum barriers [11]. To address this issue, several carrier systems, such as liposomes [12], microneedles [13], lipid vesicles [14] and solid lipid nanoparticles (SLNs) [15], have been employed to facilitate the transdermal or dermal delivery of CyA. However, these systems are not without drawbacks. For example, nanocarriers suffer from relatively large sizes, instability, and complicated and costly preparative processes, whereas microneedles may cause potential skin damage owing to their invasive nature.

Ionic liquids (ILs) are “liquid salts” synthesized from a pair of acids and bases, one of which should be a weak one, with a melting point below 100 °C and preferably at room temperature. ILs have been utilized as solubilizers [16–18], bacteriostatic agents [19, 20], and penetration enhancers [21–24] for versatile biomedical purposes. If one of the acid/base pairs is an active pharmaceutical ingredient (API), that IL can be defined as an API-IL [25, 26]. In previous studies, enhanced dermal delivery of a series of biomacromolecules has been observed with several choline-based ILs, such as choline malate (dextran, MW 4000 g/mol) [27], choline geranate (bovine serum albumin, MW ≈ 66000 g/mol; ovalbumin, MW ≈ 45000 g/mol; and insulin, MW 5807.7 g/mol) [28], and several choline-fatty acids (peptides, MW 963.1 g/mol) [29]. ILs are emerging as a new class of permeation enhancers with promising characteristics, such as biocompatibility, degradability, tailor-made properties, stability, and safety [21–24].

In this study, ILs were utilized as both a carrier system and a permeation enhancer to enhance the permeation of CyA into the skin. Four choline-based ILs, namely, choline citrate ([Ch][Ci]), choline geranate ([Ch][Ge]), choline sorbate ([Ch][So]), and choline ricinoleate ([Ch][Ra]), were synthesized and evaluated for their potential for dermal delivery of CyA. An imiquimod (IMQ)-induced mouse psoriasis model was used to assess the efficacy of CyA-loaded ILs by evaluating psoriasis area severity index (PASI) scores, spleen weight, histopathological changes, and the levels of key inflammatory cytokines, including tumor necrosis factor (TNF)- α , interleukin (IL)-17, and IL-22.

Materials and methods

Materials

CyA was a kind gift from the Sichuan Industrial Institute of Antibiotics (Chengdu, China). Acetonitrile and methanol were acquired from CINC High Purity Solvent Co. (Shanghai, China). Choline bicarbonate and 40% formalin were acquired from Sigma–Aldrich Co. (Darmstadt, Germany). *Tert*-butyl methyl ether was purchased from Aladdin Co. (Shanghai, China). Phosphoric acid was acquired from MACKLIN reagent (Shanghai, China). Geranic acid and ricinoleic acid were acquired from RHAWN Co. (Shanghai, China). Sorbic acid, citric acid, and ethanol were acquired from Sinopharm Chemical Reagent Co., Ltd. (Shanghai, China). IMQ cream was purchased from Med Shine Co. (Chengdu, China). Neoral[®], a Novartis (Basel, Switzerland) product, and betamethasone cream, a United Laboratories (Hong Kong, China) product, were purchased from a local pharmacy. A Cell Counting Kit-8 (CCK-8) was purchased from Beyotime Co. (Shanghai, China). Reagent-grade deionized water was obtained *via* a Milli-Q purification system (Millipore, MA, USA). All remaining reagents were of analytical grade.

BALB/c mice (18–20 g) and SD rats (150–200 g) were purchased from Shanghai Laboratory Animal Center (China) and raised at the Experimental Animal Center of the School of Pharmacy, Fudan University. Human immortalized epidermal cells (HaCaT cells) were purchased from the National Collection of Authenticated Cell Cultures. The animal experiments were approved by the Laboratory Animal Ethics Committee of Fudan University School of Pharmacy (Protocol code 2020-040YJ-QJP-01).

Preparation and characterization of ILs

ILs were prepared via an acid–base neutralization reaction according to a previous method [27]. In brief, citric acid, geranic acid, sorbic acid, or ricinoleic acid was dissolved in 25 mL of ethanol, gradually added to a flask containing 0.05 mol of choline bicarbonate, and then stirred overnight at 25 °C. Ethanol and water were removed by vacuum rotary evaporation (60 °C for 2 h), and an IL with a low water content (below 10%, w/w) was obtained through vacuum freeze-drying for 3 h. These ILs were named after the base choline and each of the acids—[Ch][Ci] (choline citrate), [Ch][Ge] (choline geranate), [Ch][So] (choline sorbate), and [Ch][Ra] (choline ricinoleate). The water content was determined *via* a Karl Fischer moisture titrator (Kyoto Electronics, Japan). In brief, before the experiment, anhydrous methanol and Karl Fischer reagent were added to the instrument, and the instrument was subsequently calibrated

with pure water. After calibration, 1 mL of different ILs was added to the instrument. The water content was calculated by the consumption of the reagent. The viscosity was assessed with a rotational rheometer (Malvern, U.K.) and calculated by measuring the shear rate and shear stress.

Quantification of CyA

The quantification of CyA was performed *via* high-performance liquid chromatography (HPLC) with Agilent 1260 equipment according to a previous method [2]. The mobile phase was a mixture of acetonitrile, water, *tert*-butyl methyl ether, and phosphoric acid (60:35:5:0.1, v/v/v/v). A C₁₈ column (Agilent, Zorbax SB, 5 μm, 4.6 mm × 250 mm) was utilized to separate CyA. The detection wavelength was 210 nm. The flow rate was kept constant at 1.5 mL/min, while the column temperature was kept at 70 °C. Samples with a volume of 20 μL were injected for analysis.

Solubility of CyA in ILs

The solubility of CyA was determined *via* a modified equilibrium method [30]. Briefly, CyA was dissolved in 10 mL of ethanol, and an excess amount of CyA was added to 1 mL of each formulation. The ethanol was removed by vacuum rotary evaporation at 60 °C for 2 h. The mixtures were mechanically shaken for 24 h at room temperature (20 °C) to ensure solubility equilibrium, followed by centrifugation at 13,000 rpm for 20 min to remove the undissolved precipitate. The amount of CyA in the supernatant was then determined *via* high-performance liquid chromatography (HPLC) following appropriate dilution with the mobile phase.

Preparation of CyA-loaded ILs

The CyA-loaded ILs (CyA-ILs) were simply obtained by adding a CyA ethanol solution to the ILs through vortex mixing followed by vacuum rotary evaporation to remove ethanol. The concentration of CyA in the ILs was fixed at 5 mg/mL (0.5%, w/w) according to the topical dosage of CyA [12, 15]. To evaluate the influence of water content on penetration efficacy, CyA-ILs with different water contents were prepared. The blank control consisted of a suspension of CyA in phosphate-buffered saline (PBS) at a concentration of 5 mg/mL (0.5%, w/w). The positive controls were a solution of CyA in 20% DMSO and Neoral[®] (CyA dissolved in a solution of ethanol, propylene glycol, glycerol and macroglycerol hydroxystearate) diluted with PBS to the same CyA concentration.

Stability of CyA in ILs

The chemical stability of CyA in the ILs was evaluated by measuring the CyA content, while its conformational stability was assessed by circular dichroism (CD) spectroscopy (Applied Photophysics Chirascan Spectrometer, Surrey, UK) [31]. For CD analysis, CyA-ILs were diluted to a concentration of 50 μg/mL in PBS containing 25% ethanol, and a CyA solution in PBS with 25% ethanol at the same concentration was used as a control. Spectra were collected in the far-UV range (190–250 nm) using a cell with a path length of 0.5 mm and a time interval of 0.5 s. Each sample was detected in triplicate. Chirascan software (version 4.2.17) was used to estimate the content of the secondary structure.

In vitro release of CyA from ILs

A Franz diffusion cell (Kaikai Technology Trade Co., Shanghai, China) with an effective diffusion area of 1.77 cm² was utilized to evaluate the *in vitro* release of CyA from ILs. A dialysis membrane (MWCO 1500, Spectrum, USA) was mounted between the donor and receptor chambers, and 7 mL of PBS (pH = 7.4) containing 25% ethanol was used as the receptor medium. CyA-loaded ILs and CyA solution dissolved in the receptor medium (0.5 mL, equivalent to 2.5 mg of CyA) were added to the donor chamber, and the medium in the receptor chamber was stirred at 500 rpm and maintained at 32 °C. At predetermined time intervals (0.083, 0.25, 0.5, 1, 2, 4, 6, 8, and 12 h), 500 μL of the sample from the receptor chamber was withdrawn, and an equivalent amount of fresh receptor medium at the same temperature was replenished. The CyA content was analyzed *via* HPLC as described above.

In vitro permeation into rat skin

The *in vitro* permeation profile was tested under the same experimental conditions as those used in the *in vitro* release study, including the same Franz diffusion cells, receptor medium, stirring speed, and temperature. The excised full-thickness rat abdominal skin was mounted between the donor and receptor chambers. Then, 0.5 mL of the test formulation (equivalent to 2.5 mg of CyA) was added to the donor cell. At predetermined time intervals (0.5, 1, 2, and 4 h), 0.5 mL of each sample was withdrawn and analyzed *via* HPLC, and an equal volume of fresh fluid at equal temperatures was replenished simultaneously. After 4 h, the rat skin samples were removed, washed with PBS, gently wiped with paper, and stored at −20 °C for further analysis. The amount of CyA retained in the skin tissue was analyzed according to a previous method [32]. Briefly, the skin tissue

was first cut into small pieces and mixed thoroughly following the addition of 3 mL of mobile phase. The mixture was then subjected to ultrasonic extraction at room temperature for 1 h and then centrifuged for HPLC analysis.

Mouse model and treatment

An IMQ-induced psoriasis mouse model was established *via* a previously reported method [33]. Healthy male BALB/c mice were randomly divided into 8 groups ($n=5$): PBS (normal control), IMQ-induced model, IMQ+betamethasone cream (positive control 1), IMQ+topical Neoral[®] (positive control 2), IMQ+blank ILs (negative control), and IMQ+CyA-loaded ILs with different water contents (10%, 20%, and 30%). Briefly, a 2.5 cm × 2.5 cm area on the back of each mouse was depilated with a Vetin Depilatory Cream one day prior to the study. With the exception of the PBS group, 62.5 mg of IMQ cream was applied to each mouse back once daily for seven consecutive days. Six hours after IMQ application, 100 μ L of different CyA formulations (5 mg/mL, equivalent to 25 mg/kg CyA) and betamethasone cream (20 mg for each mouse, equivalent to 1 mg/kg betamethasone) were applied throughout the entire administration area. Formulations with high viscosities could be well retained on skin surfaces and were painted directly on the target area. Only diluted IL formations with 20% and 30% water content and PBS could not be well retained and therefore were carefully painted multiple times, with a small amount of the formulation each time. The body weight of each mouse was recorded daily during the experiment. At the end of the experiment, the PASI score was determined via a four-point scale ranging from none (0) to very severe (4) on the basis of the intensity of redness, scaling conditions, and thickness of the skin, according to previous methods [34–36]. After euthanization *via* decapitation, the skin and spleen tissues were collected for further evaluation.

Hematoxylin and eosin staining

The skin tissue samples from the animal treatment study were embedded in paraffin and cut into 5 μ m-thick slices *via* a microtome (Leica, Germany), after which hematoxylin and eosin (HE) staining was performed. The tissue sections were observed with an Olympus VS200 full-glass scanner (Olympus, Japan) to identify signs of increased epidermal thickness, inflammatory cell infiltration, and abnormal keratinocyte proliferation.

ELISA

Previous studies [12] have shown that TNF- α , IL-22 and IL-17 are typical inflammatory cytokines involved in

psoriasis. Psoriatic skin from the treatment study was excised, weighed, processed into a 10% homogenate with PBS and subjected to centrifugation at 3000 rpm for 10 min. The resulting supernatants were analyzed *via* ELISA for TNF- α , IL-22, and IL-17.

Skin irritation

Male SD rats weighing 150–200 g were separated into three groups with five mice in each group. One day prior to the study, the backs of the mice were shaved. The IL group received 100 μ L of IL ([Ch][So]) daily on the shaved area three times a day for a period of seven days, whereas the blank and positive control groups received PBS and 20% DMSO. The application sites were visually observed throughout the experiment. Following euthanization, the rat skin was isolated, fixed, embedded in paraffin, and observed after HE staining.

Cytotoxicity

HaCaT cells were cultured in Dulbecco's modified Eagle's medium (DMEM) supplemented with 10% fetal bovine serum (FBS) at 37 °C in a 5% CO₂ incubator. HaCaT cells were seeded in 96-well plates at a concentration of 2×10^4 cells/well and cultured for 24 h. Then, the medium was replaced with 100 μ L of IL solutions at different concentrations. After incubation for 6 h, the cells were washed with PBS. CCK-8 was utilized to detect cell viability. Briefly, after removing the ILs, 10 μ L of CCK-8 and 100 μ L of medium were added to each well and incubated at 37 °C for 0.5 h. The absorbance at 450 nm of each well was measured with a Synergy 2 microplate reader (Bio-Tek, USA) to calculate the cell viability.

In vivo TEWL assay

Trans-epidermal water loss (TEWL) is the process of passive water diffusion through the skin, reflecting its ability to function as a barrier to water movement [37]. The animal grouping and sample preparation for TEWL assessment were conducted in the same manner as described for skin irritation. The initial TEWL of the shaved site was measured *via* a vacuum evaporimeter (Delfin, Finland) 1 h prior to the experiment. During the experiment, 100 μ L of each test sample was applied to the entire treatment area at 15-min intervals. One hour after administration, the test areas were washed with PBS and dried. TEWL was measured at 0, 0.5, 1, 2, and 4 h post administration.

Data analysis

The data were analyzed *via* Origin Pro 2024 and are presented as the means \pm SDs. Comparisons between groups were assessed by independent sample *t* tests and one-way analysis of variance *via* IBM SPSS statistics 25. Statistical significance is presented as * $P < 0.05$, ** $P < 0.01$, and *** $P < 0.001$.

Results and discussion

Characterization of ILs and CyA-ILs

The four choline-based ILs listed in Table 1 were synthesized according to the synthetic scheme (Fig. 1a). Since the structures of these ILs were identified in our previous studies [18, 27], we did not carry out repetitive identification in this study. Only the appearance, water content and viscosity were characterized. As shown in Fig. 1b, the ILs were clearly transparent liquids. After freeze-drying, the water content of the four ILs could be reduced to less than 10%, which might not significantly affect the ionic interactions in ILs according to previous experience [38]. The chain length and number of carboxyl groups in the aliphatic acids strongly affected the viscosity of the ILs. [Ch][Ra] exhibited the highest viscosity, which may be due to its long side chains, whereas the higher viscosity of [Ch][Ci] may be associated with the multiple carboxyl groups in citric acid. With a single carboxyl group and a shorter side chain, either [Ch][Ge] or [Ch][So] has a lower viscosity. This difference may be due to more complicated entanglement in ILs with more carboxyl groups and longer side chains.

The solubilization of CyA in water by ILs was evaluated. An HPLC method was first developed for the determination of CyA (Fig. S1). As shown in Fig. 1c, the solubility of CyA in three of the four ILs reached approximately 95.5 mg/mL, which was 8.8 times greater than that of the 20% DMSO control group (10.8 mg/mL). However, the solubility of CyA in [Ch][Ci] was only 16.4 mg/mL, which was slightly greater than that of the DMSO group. With increasing water content

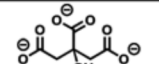
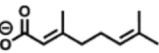
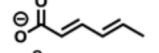
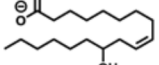
in the ILs, the solubility of CyA decreased significantly, but [Ch][Ge] and [Ch][Ra] with a water content of 70% still had a considerable ability to solubilize CyA, which was not significantly different from that of the DMSO group (Fig. 1d). In addition, the stability of CyA in the ILs was evaluated. Owing to the limited solubility of CyA in [Ch][Ci], only [Ch][Ge], [Ch][So], and [Ch][Ra] were tested. The content of CyA in the three ILs remained stable for up to seven days (Fig. 1e), which ensures stability during the efficacy experiments over the same period. CD spectroscopy verified the stability of the secondary structure of CyA (Fig. 1f). The negative absorption peak at approximately 226 nm in the CD spectrum indicates the typical structural features of the β -turn in CyA [31]. Figure 1f clearly shows identical CyA absorption peaks in both the ILs and the PBS solution containing 25% ethanol, suggesting the conformational stability of CyA in the ILs. In summary, [Ch][Ge], [Ch][So] and [Ch][Ra] could significantly improve the solubility of CyA and were therefore selected for downstream studies.

In vitro penetration of CyA

In vitro penetration of CyA was evaluated in excised rat abdominal skin. In our preliminary study, CyA could not be detected in the receiving chamber until 8 h, indicating negligible penetration of CyA through intact skin. Therefore, the retention of CyA in the skin tissue was evaluated, and the in vitro penetration time was shortened to 4 h to ensure that the data were collected from intact skin. As shown in Fig. 2a, compared with the negative control and DMSO, all three ILs significantly enhanced the dermal delivery of CyA. Among all ILs, [Ch][Ge] displayed the best dermal delivery ability, followed by [Ch][So] and [Ch][Ra].

The water content of ILs significantly influences their ability to enhance dermal penetration [27, 38], so ILs with different water contents were evaluated. As the water content in the ILs increased from 10 to 70%, the dermal deposition of CyA first increased, peaked at a water content of 30%, and then decreased significantly. In the [Ch][Ge] and [Ch][Ra] groups with a water content of 70%, the dermal deposition of CyA was still comparable to that

Table 1 Structures and physical properties of choline-based ILs

ILs	Anion	Molar ratio (cation/anion)	Water content (% w/w)	Viscosity (Pa·S)
Choline/citric acid [Ch][Ci]		3:1	7.92	8.65 \pm 0.55
Choline/geranic acid [Ch][Ge]		1:1	8.81	1.86 \pm 0.04
Choline/sorbic acid [Ch][So]		1:1	7.61	3.31 \pm 0.23
Choline/ricinoleic acid [Ch][Ra]		1:1	6.36	13.97 \pm 0.60

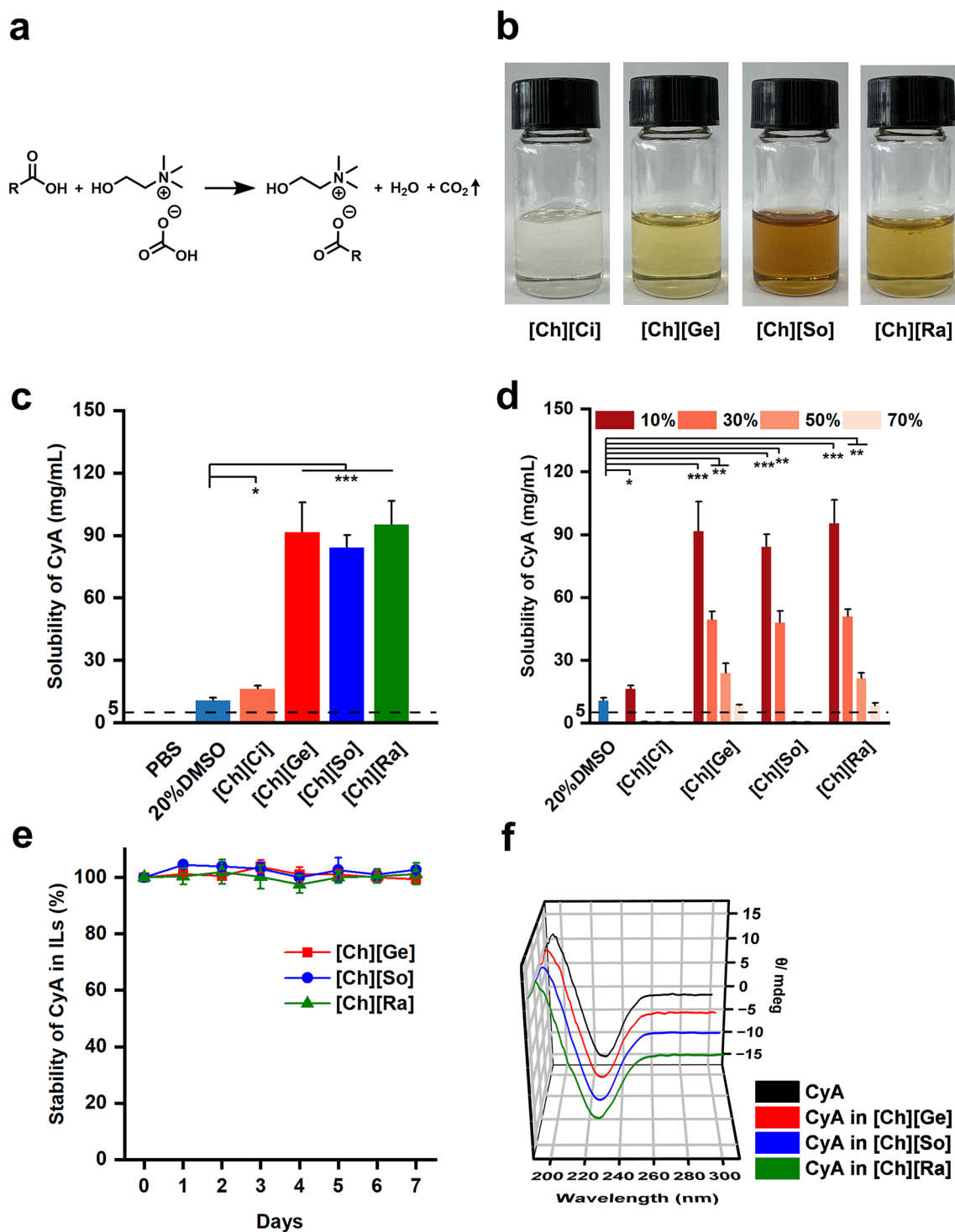


Fig. 1 Synthesis and characterization of ILs and CyA-loaded ILs. **(a)** Synthesis of choline-based ILs by using choline bicarbonate as the base. The types of acids (R-) and molar ratios of the reactions are shown in Table 1. **(b)** The appearance of the ILs. **(c)** Solubility of CyA in PBS, 20% DMSO and different ILs. **(d)** Solubility of CyA in 20% DMSO and ILs with different water contents (10%, 30%, 50%, and

70%). A water content of 10% represented undiluted ILs. **(e)** Changes in the content of CyA in ILs over seven days at room temperature. **(f)** Conformational stability of CyA in ILs evaluated by CD spectroscopy compared with that of CyA in PBS containing 25% ethanol. *** $P < 0.001$; ** $P < 0.01$; * $P < 0.05$. $n = 3$

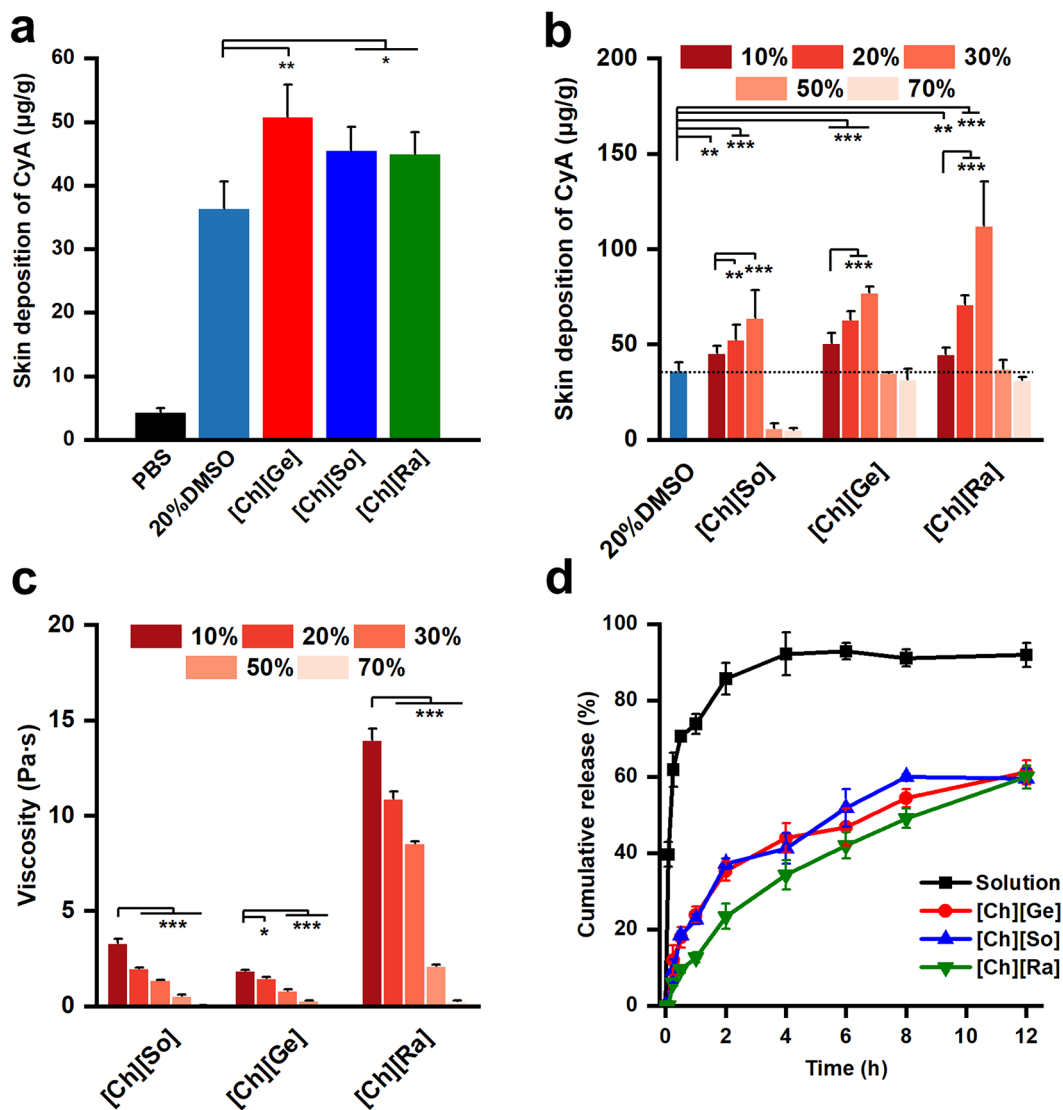


Fig. 2 In vitro evaluation of the enhanced dermal delivery of CyA by ILs. **(a)** In vitro permeation of CyA into rat skin in the presence of PBS, 20% DMSO or different ILs (CyA/skin, µg/g). **(b)** Enhanced in vitro permeation of CyA into rat skin by ILs with different water contents (10%, 20%, 30%, 50%, and 70%). A water content of 10%

represented undiluted ILs. **(c)** Viscosities of ILs with different water contents (10%, 20%, 30%, 50%, and 70%). **(d)** In vitro release of CyA from the ILs compared with that of the CyA solution in PBS containing 25% ethanol. *** $P < 0.001$; ** $P < 0.01$; * $P < 0.05$. $n = 3$

in the DMSO group. However, the dermal delivery efficiency of CyA in [Ch][So] with a water content above 50% was very low, which may be due to the limited solubilization ability of [Ch][So] at such a high water content (Fig. 1d).

The penetration-enhancing ability of ILs is affected not only by the type of ILs but also by the interactions between drugs and ILs. When the ILs were slightly diluted, the viscosity of the ILs decreased, leading to accelerated release of CyA from the ILs. On the other hand, slight dilution did not significantly affect the penetration-enhancing ability of the ILs, thus resulting in enhanced penetration of more CyA by slightly diluted ILs. With a further increase in water

content, the structure of the ILs may deteriorate gradually [38], leading to a decrease in their penetration-enhancing ability. Consequently, ILs containing 30% water exhibited optimal dermal delivery of CyA. Concurrent determination of viscosity indicated significantly decreased viscosity as a result of dilution by water (Fig. 2c). CyA was released more slowly than it was from PBS containing 25% ethanol (Fig. 2d). The release of CyA in the PBS group reached a maximum at 4 h, whereas only 60% of the CyA-loaded ILs were released at 12 h. Additionally, the release of CyA from [Ch][Ra] was slower than that from the other two ILs, which could be attributed to the higher viscosity of [Ch][Ra].

Efficacy

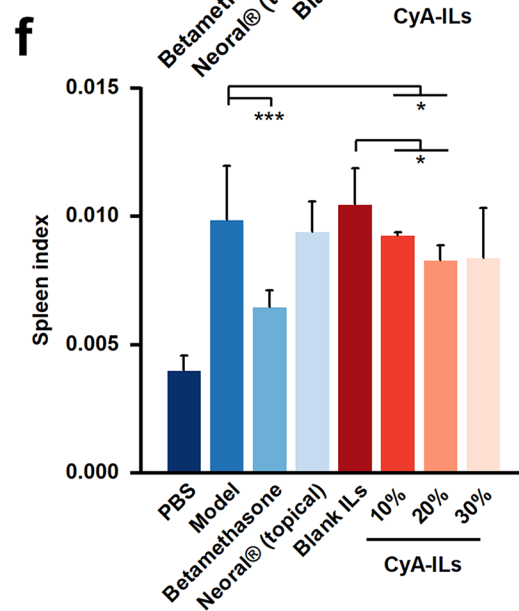
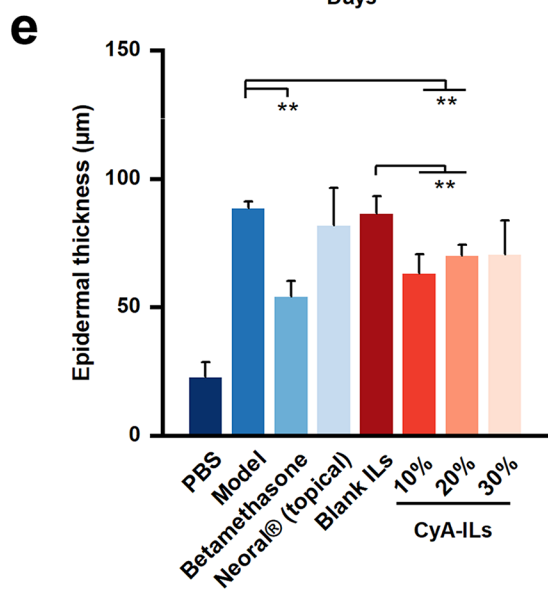
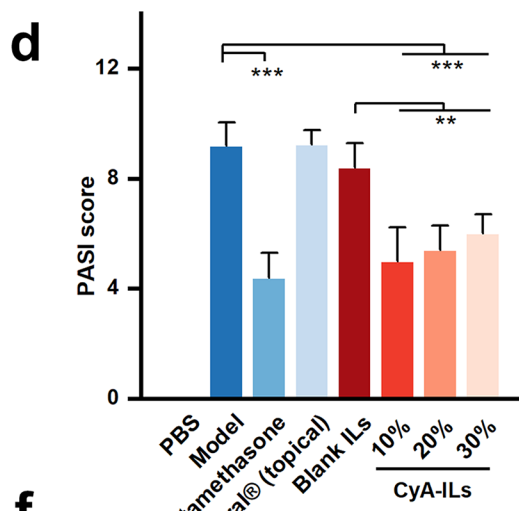
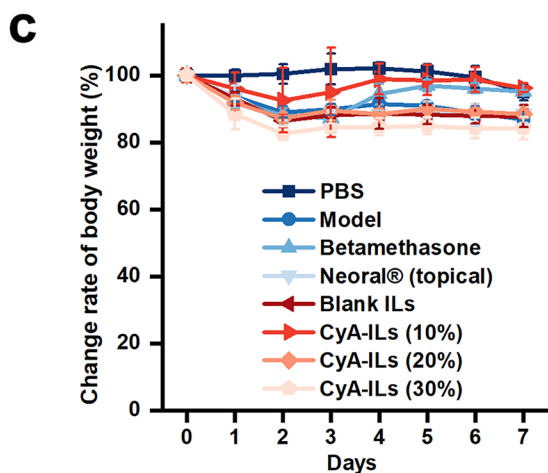
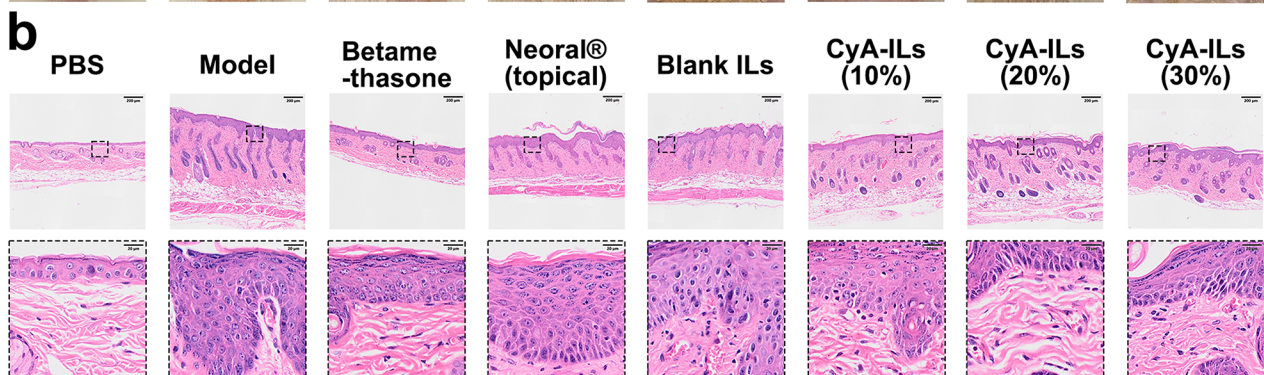
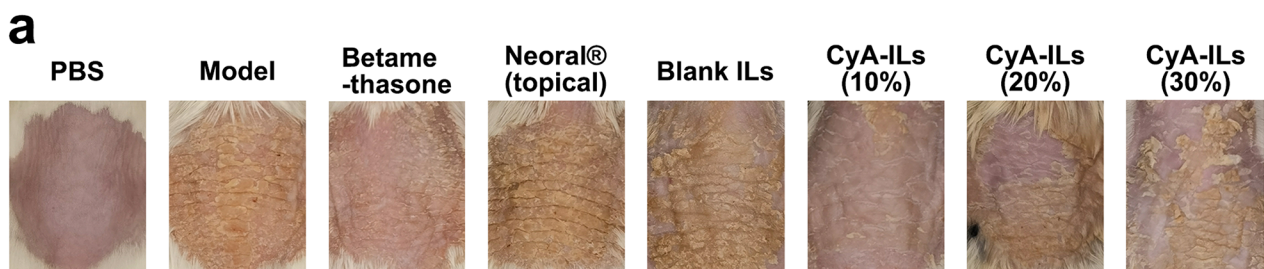
An IMQ-induced psoriasis mouse model was established to evaluate the efficacy of the topical administration of CyA-loaded ILs. As [Ch][So], [Ch][Ge], and [Ch][Ra] all displayed excellent dermal penetration of CyA in vitro, they were further optimized in vivo. Among the three ILs, one mouse in the [Ch][Ge] group died on the first day, whereas the others demonstrated subcutaneous hemorrhage (Fig. S2b) and died on day 4. As direct administration of both CyA and the blank [Ch][Ge] did not result in obvious toxicity, the current observations looked unexplainable. Although the exact reason for the death and severe toxicity of the experimental animals has yet to be elucidated, the interplay of CyA and [Ch][Ge] may play a role and lead to lethal outcomes. Alternatively, there might also be unknown synergy between [Ch][Ge] and CyA or unpredictable events such as rapid and substantial absorption in vivo, which, however, has yet to be elucidated. Importantly, care should be taken when [Ch][Ge] is used as a permeation enhancer. The mice in the [Ch][Ra] group presented obvious skin irritation and psoriasis characteristics (Fig. S2c). This may be attributed to the longer side chain of [Ch][RA], which deteriorates the lipid layers in the stratum corneum [39]. Therefore, only [Ch][So] was chosen for downstream evaluations. Considering the low solubilization and penetration-enhancing ability at a water content above 50%, the water content was set at 10%, 20% and 30%.

After seven days of continuous IMQ treatment, the psoriasis-like mouse model was successfully established (Fig. 3a). Body weight monitoring revealed a decrease in body weight during the initial four days (Fig. 3c), which was likely caused by the inflammatory response induced by IMQ. The blank ILs caused almost no alleviation of psoriatic symptoms, but the scaling conditions were ameliorated, indicating a softening effect on the stratum corneum (Fig. 3a). The mice in the CyA-loaded IL group presented milder psoriatic symptoms, which were not significantly different from those in the positive control group (betamethasone), with reduced erythema and scaling. Notably, the water content in the ILs did not influence the therapeutic effect. Although slightly diluted ILs may enhance the in vitro dermal deposition of CyA (Fig. 2b), a decrease in viscosity shortens the retention time of CyA on the skin, thereby impacting its therapeutic efficacy. Surprisingly, the Neoral[®] group showed no alleviation of psoriatic characteristics, as judged by appearance. The PASI showed the same trend for each group (Fig. 3d). Compared with those of the model group, the betamethasone and IL groups presented notable decreases in spleen weight (Fig. 3f), indicating decreases in inflammation and psoriatic symptoms [12, 40]. HE staining was performed to assess histopathological changes and epidermal thickness

Fig. 3 Topical treatment of psoriatic mice. The groups were categorized as follows: blank control (PBS), positive control (betamethasone), positive control (Neoral[®]), negative control (blank ILs), and treatment groups (CyA-ILs with water contents of 10%, 20% and 30%). A water content of 10% represented undiluted ILs. During the seven-day experiment, IMQ was applied to the shaved area on the backs of the mice every morning to induce psoriasis. Four hours after modeling, the mice were treated with 100 μ L of PBS or a diluted solution of Neoral[®] or ILs in the shaved area at a CyA dosage of 25 mg/kg. The dosage of betamethasone was set at 1 mg/kg. **(a)** Appearance of psoriasis-like skin on day 7. **(b)** HE-stained images of psoriasis-like skin on day 7 (the scale bar represents 200 μ m for the original image and 20 μ m for the enlarged image). **(c)** Changes in body weight over 7 days. **(d)** PASI scores of psoriasis-like skin. **(e)** Epidermal thickness calculated from HE-stained images. **(f)** Spleen index = spleen weight/body weight. *** $P < 0.001$; ** $P < 0.01$; * $P < 0.05$. $n = 5$

(Fig. 3b and e). CyA-loaded IL treatment reduced epidermal thickening and hyperkeratosis. As the water content increased from 10 to 30%, the thickness of the epidermis slightly increased.

The overexpression of TNF- α , IL-22 and IL-17 leads to persistent inflammation and excessive proliferation of keratinocytes in psoriasis, whereas the calcineurin inhibitor CyA can effectively inhibit T-cell activation, resulting in decreased levels of these inflammatory factors [41–43]. Therefore, the three inflammatory factors were tested to further evaluate their therapeutic effects. As shown in Fig. 4, the levels of TNF- α , IL-22 and IL-17 in the model group were five times greater than those in the healthy (PBS) group, whereas the undiluted IL group presented a 71.7% reduction in TNF- α , a 75.6% reduction in IL-22, and an 89.3% reduction in IL-17, which were also greater than those in the betamethasone group. Blank ILs and the water content of the ILs had no significant effect on the cytokine levels. The Neoral[®] group also demonstrated a reduction in cytokine levels, indicating facilitated absorption of CyA. The presence of various emulsifiers and coemulsifiers in the formulation may function as permeation enhancers. Compared with previous studies, ILs achieved comparable efficacy in enhancing the dermal delivery of CyA to that achieved with nanocarriers [13–15] while exhibiting superior performance in reducing cytokine levels [12]. As nanocarrier systems are associated with various problems, such as complicated preparative processes, instability, poor reproducibility, and difficulties in translation, ILs prove to be more promising delivery systems for enhanced dermal drug delivery with prestigious features of solubilization, penetration enhancement, and tailorable viscosity that facilitate formulation and easy administration.



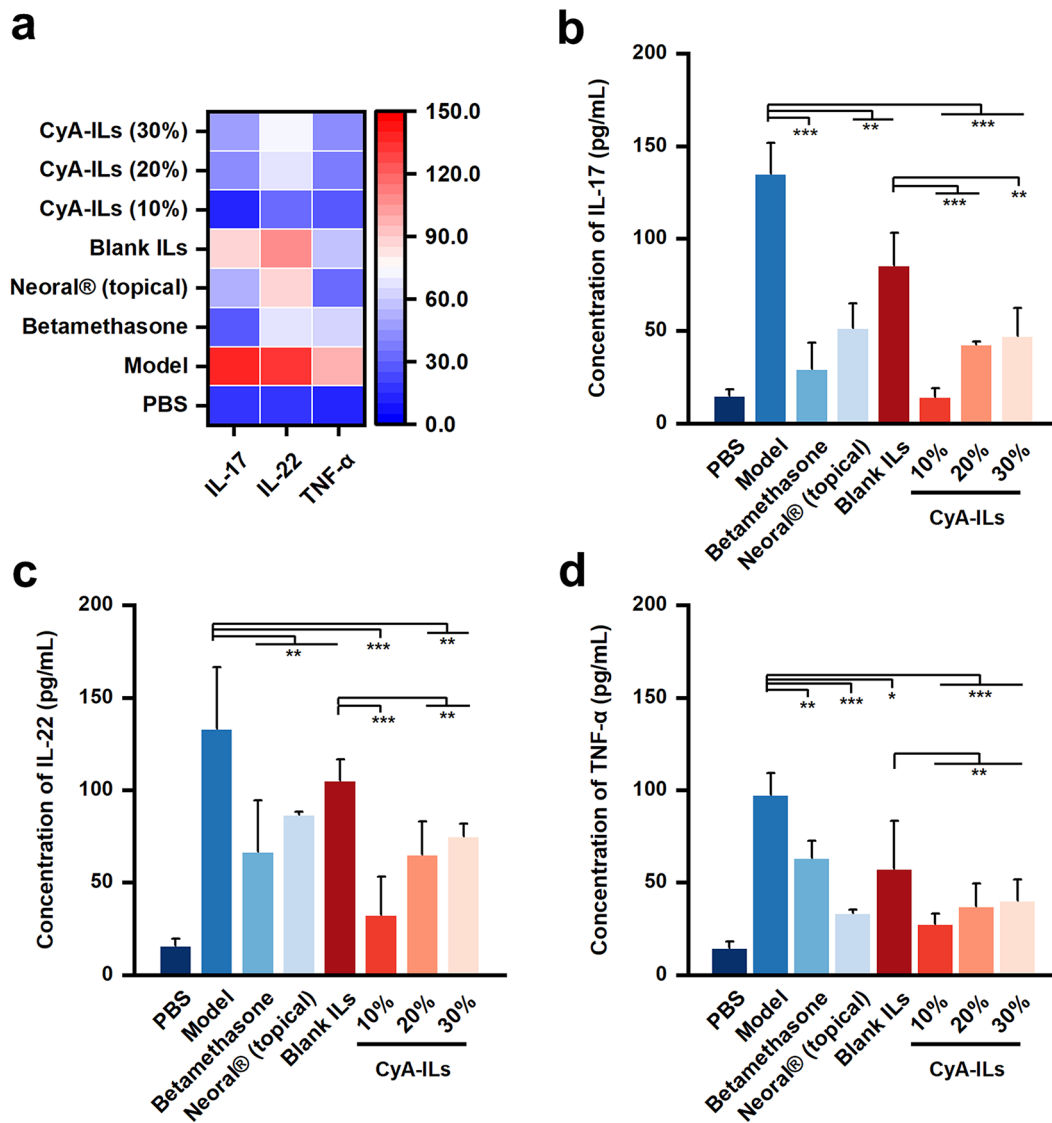


Fig. 4 Inflammatory cytokine levels in a mouse psoriasis model after treatment. On day 7, the psoriasis-like skin was removed, and ELISA was performed. (a) Heatmap of three inflammatory cytokines in differ-

ent groups and the quantified levels of IL-17 (b), IL-22 (c) and TNF- α (d). *** $P < 0.001$; ** $P < 0.01$; * $P < 0.05$. $n = 5$

Safety evaluation

Cytotoxicity, TEWL and histological variations were observed to test the safety of ILs applied to the skin. Cytotoxicity was assessed in HaCaT cells, which are commonly used as cell models for transdermal drug delivery [44], via the CCK-8 method for evaluating cell viability [45]. The cell viability decreased as the concentration of the IL ([Ch][So]) increased, with an IC_{50} value of 148.64 ± 10.96 mmol/L (Fig. 5b), in contrast with the IC_{50} of 0.20 ± 0.02 mmol/L reported for azone [46], a widely used chemical penetration enhancer. [Ch][So] showed significantly reduced cytotoxicity in comparison with azone. TEWL is an indirect index that reflects the

influence on the integrity of skin barriers [47]. Compared with the blank group (PBS), both the positive control (20% DMSO) and the IL ([Ch][So]) exhibited significantly increased TEWL within 1 h after administration (Fig. 5d), which was consistent with the drug permeation results because a higher TEWL value is usually related to enhanced drug penetration. After removal of the test samples, the TEWL gradually decreased and returned to its initial level within 2 h, indicating that [Ch][So] could effectively moderate the skin barriers in a reversible manner.

According to the histological images (Fig. 5c), the epidermal layer appeared to be significantly thicker in the DMSO group than in the control group, with a noticeable

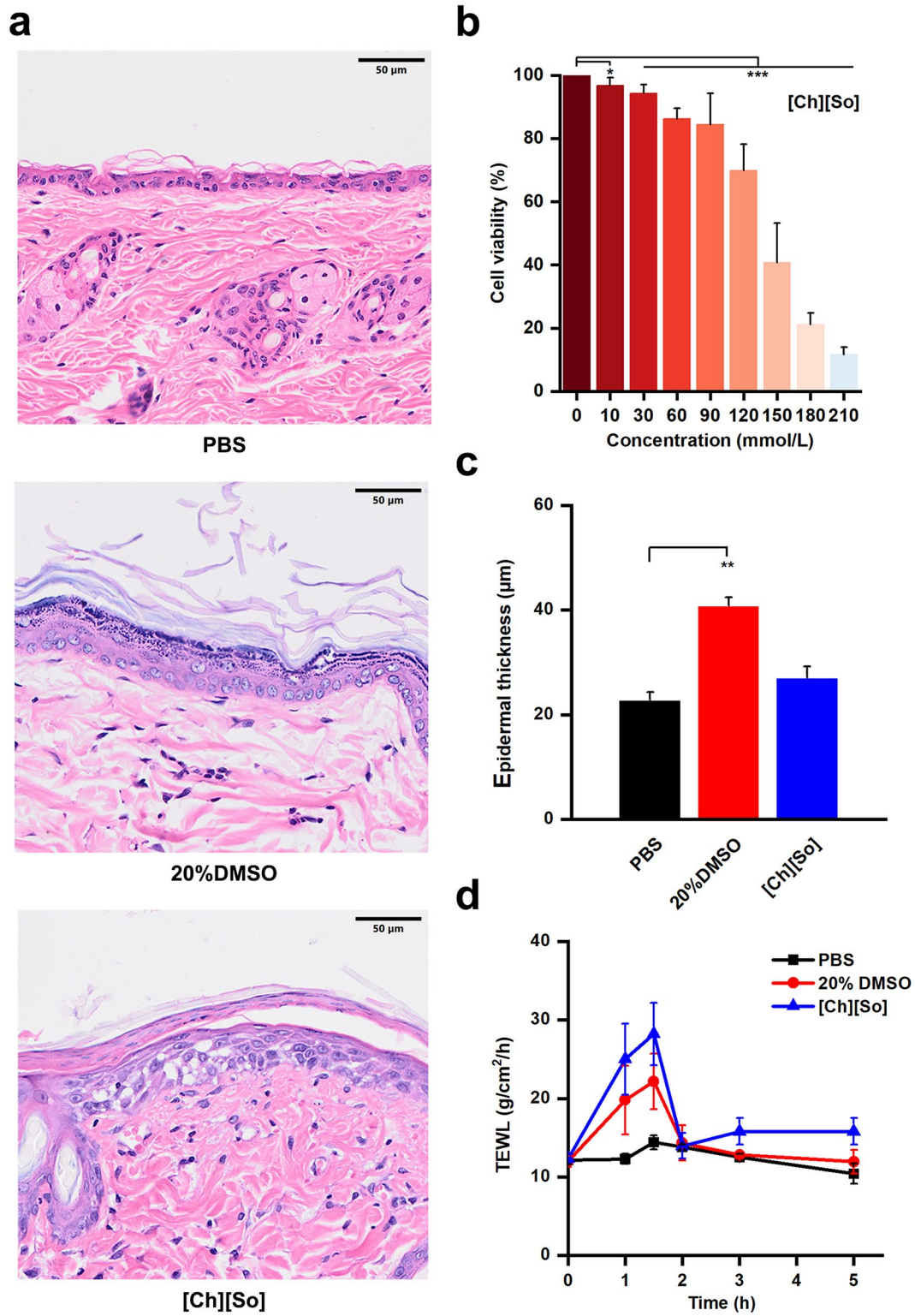


Fig. 5 Safety evaluation of [Ch][So] in HaCaT cells and SD rats. (a) Histological sections of rat skin treated with PBS, 20% DMSO, or [Ch][So]. (b) Viability of HaCaT cells after coculture with different concentrations of [Ch][So]. (c) Epidermal thickness calculated

from histological sections of rat skin. (d) TEWL values of rat skin treated with PBS, 20% DMSO, or [Ch][So]. *** $P < 0.001$; ** $P < 0.01$; * $P < 0.05$. The scale bar represents 50 µm. $n = 5$

phenomenon of keratinocyte detachment, indicating skin irritation. In contrast, the degree of epidermal layer thickening in the [Ch][So] group was obviously lower than that in the DMSO group, and there were no signs of edema or inflammatory infiltration. These findings suggested that [Ch][So] could serve as a safe and reliable penetration enhancer.

Conclusion

The four synthesized choline-based ILs, i.e., [Ch][Ci], [Ch][Ge], [Ch][So], and [Ch][Ra], all appear to be viscous, transparent liquids with water contents less than 10%. A longer chain length ([Ch][Ra]) and multiple carboxyl groups ([Ch][Ci]) of the aliphatic acid are associated with a higher viscosity of the ILs. The functions of ILs include various aspects. ILs can serve as formulation vehicles with a CyA solubility of more than 90 mg/mL, in which CyA can remain stable both chemically and structurally. An *in vitro* penetration study revealed negligible transport of CyA across excised rat abdominal skin. Compared with that of PBS and DMSO, the skin deposition of CyA by ILs significantly increased in the order of [Ch][Ge] > [Ch][So] > [Ch][Ra]. An *in vivo* efficacy test demonstrated that CyA-loaded [Ch][So] cream significantly reduced psoriatic features, epidermal thickness, and TNF- α , IL-22 and IL-17 levels in the skin to a greater extent than did the positive control betamethasone cream. The effects of the water content of the ILs on their performance were confirmed by both *in vitro* and *in vivo* investigations. Despite the ameliorating effect of water, [Ch][Ge] and [Ch][Ra] with a water content of 70% could still have a considerable solubilization capability for CyA. Compared with undiluted ILs, diluted ILs with a water content of 30% showed greater permeation ability, which may be related to the lower viscosity of the diluted ILs, which resulted in faster drug release from the IL carriers. Furthermore, [Ch][So] exhibited lower cytotoxicity than azone did, and it did not induce significant irritation after 7 days of skin application. Multiple mechanisms may be involved in the enhanced dermal delivery of CyA by ILs, including (1) serving as a solubilizer for CyA, (2) softening the scaling skin surfaces, and (3) interfering with the lipid matrices of the skin or extracting lipids from the formulations. It has been concluded that choline-based ILs function to increase the permeation and retention of CyA in the skin, which holds promise for the potential treatment of psoriasis.

Supplementary Information The online version contains supplementary material available at <https://doi.org/10.1007/s13346-024-01705-8>.

Author contributions All the authors contributed to the study conception and design. Material preparation, data collection and analysis were performed by Yang Li and Qin Yu. The first draft of the manuscript was written by Yang Li, and all the authors commented on previous versions of the manuscript. All the authors read and approved the final manuscript.

Funding The authors declare that no funds, grants, or other support was received during the preparation of this manuscript.

Data availability The datasets generated during and/or analyzed during the current study are available from the corresponding author upon reasonable request.

Declarations

Ethics approval All institutional and national guidelines for the care and use of laboratory animals were followed. The animal protocol of this study was approved by the institutional ethical committee of the School of Pharmacy, Fudan University (2020-040YJ-QJP-01).

Consent to participate Not applicable.

Consent for publication Not applicable.

Competing interests The authors have no relevant financial or non-financial interests to disclose.

References

- Zhu B, Jing M, Yu Q, Ge X, Yuan F, Shi L. Treatments in psoriasis: from standard pharmacotherapy to nanotechnology therapy. *Adv Dermatol Allergol*. 2022;39:460–71.
- Wang K, Qi J, Weng T, Tian Z, Lu Y, Hu K, Yin Z, Wu W. Enhancement of oral bioavailability of cyclosporine A: comparison of various nanoscale drug-delivery systems. *Int J Nanomed*. 2014;9:4991–9.
- Bos JD, Spuls PI. Topical treatments in psoriasis: today and tomorrow. *Clin Dermatol*. 2008;26:432–7.
- Rosmarin DM, Lebwohl M, Elewski BE, Gottlieb AB. National psoriasis F. Cyclosporine and psoriasis: 2008 national psoriasis foundation consensus conference. *J Am Acad Dermatol*. 2010;62:838–53.
- Lee HJ, Kim M. Challenges and future trends in the treatment of psoriasis. *Int J Mol Sci*. 2023;24:13313.
- Reid C, Griffiths CEM. Psoriasis and treatment: past, present and future aspects. *Acta Derm Venereol*. 2020;100:5649.
- Patel D, Wairkar S. Recent advances in cyclosporine drug delivery: challenges and opportunities. *Drug Deliv Transl Res*. 2019;9:1067–81.
- Bhardwaj P, Tripathi P, Pandey S, Gupta R, Ramchandra Patil P. Cyclosporine and pentoxifylline laden tailored niosomes for the effective management of psoriasis: *in vitro* optimization, *ex-vivo* and animal study. *Int J Pharm*. 2022;626:122143.
- Gomes GS, Frank LA, Contri RV, Longhi MS, Pohlmann AR, Guterres SS. Nanotechnology-based alternatives for the topical delivery of immunosuppressive agents in psoriasis. *Int J Pharm*. 2023;631:122535.
- Li N, Qin Y, Dai D, Wang P, Shi M, Gao J, Yang J, Xiao W, Song P, Xu R. Transdermal delivery of therapeutic compounds with nanotechnological approaches in psoriasis. *Front Bioeng Biotechnol*. 2021;9:804415.

11. Romero GB, Arntjen A, Keck CM, Muller RH. Amorphous cyclosporin A nanoparticles for enhanced dermal bioavailability. *Int J Pharm.* 2016;498:217–24.
12. Walunj M, Doppalapudi S, Bulbake U, Khan W. Preparation, characterization, and in vivo evaluation of cyclosporine cationic liposomes for the treatment of psoriasis. *J Liposome Res.* 2020;30:68–79.
13. Jeong HR, Kim JY, Kim SN, Park JH. Local dermal delivery of cyclosporin A, a hydrophobic and high molecular weight drug, using dissolving microneedles. *Eur J Pharm Biopharm.* 2018;127:237–43.
14. Carreras JJ, Tapia-Ramirez WE, Sala A, Guillot AJ, Garrigues TM, Melero A. Ultraflexible lipid vesicles allow topical absorption of cyclosporin A. *Drug Deliv Transl Res.* 2020;10:486–97.
15. Trombino S, Servidio C, Lagana AS, Conforti F, Marrelli M, Cassano R. Viscosified solid lipidic nanoparticles based on naringenin and linolenic acid for the release of cyclosporine A on the skin. *Molecules.* 2020;25:3535.
16. Ali MK, Moshikur RM, Wakabayashi R, Moniruzzaman M, Kamiya N, Goto M. Biocompatible ionic liquid surfactant-based microemulsion as a potential carrier for sparingly soluble drugs. *ACS Sustainable Chem Eng.* 2020;8:6263–72.
17. Ali MK, Moshikur RM, Wakabayashi R, Moniruzzaman M, Goto M. Biocompatible ionic liquid-mediated micelles for enhanced transdermal delivery of paclitaxel. *ACS Appl Mater Interfaces.* 2021;13:19745–55.
18. Huang W, Fang Z, Zheng X, Qi J, Wu W, Lu Y. Green and controllable fabrication of nanocrystals from ionic liquids. *Chin Chem Lett.* 2022;33:4079–83.
19. Zakrewsky M, Banerjee A, Apte S, Kern TL, Jones MR, Sesto RE, Koppisch AT, Fox DT, Mitragotri S. Choline and geranate deep eutectic solvent as a broad-spectrum antiseptic agent for preventive and therapeutic applications. *Adv Healthc Mater.* 2016;5:1282–9.
20. Zakrewsky M, Lovejoy KS, Kern TL, Miller TE, Le V, Nagy A, Goumas AM, Iyer RS, Del Sesto RE, Koppisch AT, Fox DT, Mitragotri S. Ionic liquids as a class of materials for transdermal delivery and pathogen neutralization. *Proc Natl Acad Sci U S A.* 2014;111:13313–8.
21. Md Moshikur R, Chowdhury MR, Fujisawa H, Wakabayashi R, Moniruzzaman M, Goto M. Design and characterization of fatty acid-based amino acid ester as a new green hydrophobic ionic liquid for drug delivery. *ACS Sustainable Chem Eng.* 2020;8:13660–71.
22. Lu Y, Ma Y, Wu W. Ionic liquids: emerging chemical permeation enhancers. *MedComm Biomater Appl.* 2024;3:e81.
23. Zheng L, Zhao Z, Yang Y, Li Y, Wang C. Novel skin permeation enhancers based on amino acid ester ionic liquid: design and permeation mechanism. *Int J Pharm.* 2020;576:119031.
24. Tanner EEL, Ibsen KN, Mitragotri S. Transdermal insulin delivery using choline-based ionic liquids (CAGE). *J Control Release.* 2018;286:137–44.
25. Moshikur RM, Chowdhury MR, Wakabayashi R, Tahara Y, Moniruzzaman M, Goto M. Characterization and cytotoxicity evaluation of biocompatible amino acid esters used to convert salicylic acid into ionic liquids. *Int J Pharm.* 2018;546:31–8.
26. Moshikur RM, Chowdhury MR, Wakabayashi R, Tahara Y, Kamiya N, Moniruzzaman M, Goto M. Ionic liquids with N-methyl-2-pyrrolidonium cation as an enhancer for topical drug delivery: synthesis, characterization, and skin-penetration evaluation. *J Mol Liq.* 2020;299:112166.
27. Wu X, Chen Z, Li Y, Yu Q, Lu Y, Zhu Q, Li Y, An D, Qi J, Wu W. Improving dermal delivery of hydrophilic macromolecules by biocompatible ionic liquid based on choline and malic acid. *Int J Pharm.* 2019;558:380–7.
28. Banerjee A, Ibsen K, Iwao Y, Zakrewsky M, Mitragotri S. Transdermal protein delivery using choline and geranate (CAGE) deep eutectic solvent. *Adv Healthc Mater.* 2017;6:1601411.
29. Tahara Y, Morita K, Wakabayashi R, Kamiya N, Goto M. Biocompatible ionic liquid enhances transdermal antigen peptide delivery and preventive vaccination effect. *Mol Pharm.* 2020;17:3845–56.
30. Liu K, Liu W, Dong Z, Zhang L, Li Q, Zhang R, He H, Lu Y, Wu W, Qi J. Translation of ionic liquids to be enteric nanoparticles for facilitating oral absorption of cyclosporine A. *Bioeng Transl Med.* 2023;8:e10405.
31. Nakao M, Takechi-Haraya Y, Ohgita T, Saito H, Demizu Y, Izutsu KI, Sakai-Kato K. Analysis of the interaction of cyclosporine congeners with cell membrane models. *J Pharm Biomed Anal.* 2022;218:114874.
32. Elhabal SF, Abdelaal N, Al-Zuhairy SAS, Mohamed Elrefai MF, Khalifa MM, Khasawneh MA, Elsaid Hamdan AM, Mohie PM, Gad RA, Kabil SL, El-Ashery MK, Jasti BR, Elzohairy NA, Elfar N, Elnawawy T, Hassan FE, El-Nabarawi MA. Revolutionizing psoriasis topical treatment: enhanced efficacy through ceramide/phospholipid composite cerosomes co-delivery of cyclosporine and dithranol: In-Vitro, Ex-vivo, and in-vivo studies. *Int J Nanomed.* 2024;19:1163–87.
33. Sadeghi S, Kalantari Y, Seirafianpour F, Goodarzi A. A systematic review of the efficacy and safety of topical cyclosporine in dermatology. *Dermatol Ther.* 2022;35:e15490.
34. Sawyer LM, Malotki K, Sabry-Grant C, Yasmeeen N, Wright E, Sohr A, Borg E, Warren RB. Assessing the relative efficacy of interleukin-17 and interleukin-23 targeted treatments for moderate-to-severe plaque psoriasis: a systematic review and network meta-analysis of PASI response. *PLoS ONE.* 2019;14:e0220868.
35. Hesselvig JH, Egeberg A, Loft ND, Zachariae C, Kofoed K, Skov L. Correlation between Dermatology Life Quality Index and Psoriasis Area and Severity Index in patients with psoriasis treated with ustekinumab. *Acta Derm Venereol.* 2018;98:335–9.
36. Matza LS, Brazier JE, Stewart KD, Pinto L, Bender RH, Kircik L, Jordan J, Kim KJ, Mutebi A, Viswanathan HN, Menter A. Developing a preference-based utility scoring algorithm for the psoriasis area severity index (PASI). *J Med Econ.* 2019;22:936–44.
37. Gomes A, Aguiar L, Ferraz R, Teixeira C, Gomes P. The emerging role of ionic liquid-based approaches for enhanced skin permeation of bioactive molecules: a snapshot of the past couple of years. *Int J Mol Sci.* 2021;22:11991.
38. Tanner EEL, Piston KM, Ma H, Ibsen KN, Nangia S, Mitragotri S. The influence of water on choline-based ionic liquids. *ACS Biomater Sci Eng.* 2019;5:3645–53.
39. Seweryn A. Interactions between surfactants and the skin - theory and practice. *Adv Colloid Interface Sci.* 2018;256:242–55.
40. Palamara F, Meindl S, Holcman M, Luhrs P, Stingl G, Sibilia M. Identification and characterization of pDC-like cells in normal mouse skin and melanomas treated with imiquimod. *J Immunol.* 2004;173:3051–61.
41. Biswasroy P, Pradhan D, Pradhan DK, Ghosh G, Rath G. Development of betulin-loaded nanostructured lipid carriers for the management of imiquimod-induced psoriasis. *AAPS PharmSci-Tech.* 2024;25:57.
42. Jiraskova Zakostelska Z, Reiss Z, Tlaskalova-Hogenova H, Rob F. Paradoxical reactions to anti-TNFalpha and Anti-IL-17 treatment in Psoriasis patients: are skin and/or gut microbiota involved? *Dermatol Ther.* 2023;13:911–33.
43. Parab S, Doshi G. An update on emerging immunological targets and their inhibitors in the treatment of psoriasis. *Int Immunopharmacol.* 2022;113:109341.
44. Boukamp RTPP, Breitkreutz D, Hornung J, Markham A, Fusenig NE. Normal keratinization in a spontaneously immortalized aneuploid human keratinocyte cell line. *J Cell Biol.* 1988;106:761–71.

45. Cai L, Qin X, Xu Z, Song Y, Jiang H, Wu Y, Ruan H, Chen J. Comparison of cytotoxicity evaluation of anticancer drugs between real-time cell analysis and CCK-8 method. *ACS Omega*. 2019;4:12036–42.
46. Xie F, Chai JK, Hu Q, Yu YH, Ma L, Liu LY, Zhang XL, Li BL, Zhang DH. Transdermal permeation of drugs with differing lipophilicity: Effect of penetration enhancer camphor. *Int J Pharm*. 2016;507:90–101.
47. Wertz PW. Lipids and the permeability and antimicrobial barriers of the Skin. *J Lipids*, 2018 (2018) 5954034.

Publisher's note Springer Nature remains neutral with regard to jurisdictional claims in published maps and institutional affiliations.

Springer Nature or its licensor (e.g. a society or other partner) holds exclusive rights to this article under a publishing agreement with the author(s) or other rightsholder(s); author self-archiving of the accepted manuscript version of this article is solely governed by the terms of such publishing agreement and applicable law.